Novel Skid Detection Method without Vehicle Chassis Speed for Electric Vehicle

Shin-ichiro Sakai   Hideo Sado   Yoichi Hori

University of Tokyo
Department of Electrical Engineering
7-3-1 Hongo, Bunkyo, Tokyo 113-8656, Japan
sakai@hori.t.u-tokyo.ac.jp

Abstract— **Novel wheel skid detection method without chassis velocity for electric vehicle (EV) is proposed. Proposed method can sense the skid with only the values of current and rotating velocity of motor. The output torque of motor is easily comprehensible, and the proposed method utilizes this advantage of EV. Estimation of vehicle chassis velocity or wheel absolute velocity is not required. The experiments were carried out with laboratory-made electric vehicle "UOT Electric March I", and the results show the effectiveness of this method. We also carried out some simulations to discuss how to prevent the wheel skid with this skid detector.**

Keywords— **Electric Vehicle(EV), Vehicle Motion Control, Anti Skid Break System(ABS), Traction Control System(TCS)**

I. Introduction

Recently, electric vehicle (EV) has attracted great interests as a powerful solution against environmental and energy problems. These expectations have induced a great deal of research and development, intending to put EV to practical use. With improvement of motors and batteries, some EV's have already achieved enough performance, even in the comparison with internal combustion engine vehicles (ICV's).

From the viewpoint of electric and control engineering, EV has three big advantages over ICV. First advantage is the fast and precise output torque. The output torque of motor can be controlled to follow its reference value accurately, with quite short time constant like 1[ms] and much less dead time. Such torque control is available for every type of motor, direct current (DC) motor, induction machine and permanent magnet (PM) motor. This remarkable performance of torque control bases on the precise current control technique. For example, 100 [μs] or less control period is available for current control, with digital processor and power electronics devices. This advantage of EV, the fast torque response, should enhance the performance of anti skid break system (ABS) or traction control system (TCS). Note that electric motor can accelerate and decelerate the wheel continuously, only depending on the sign of reference torque value. Thus in EV, ABS and TCS can be realized with only one actuator. We have reported that slip ratio control for TCS was experimentally achieved [1].

Second, the output torque of motor is easily comprehensible. As mentioned above, the output torque of motor is controlled to follow its reference value. Hence the reference value can be used as the actual output torque value. This will be a great help for the estimation of vehicle motion, like chassis slip angle estimation [2] or maximum tire-road friction force monitoring [3] [4]. This paper also mainly studies on this advantage.

Third, individual torque of every driven wheel can be controlled independently, in such EV with in-wheel motors [5]. IZA [6] is equipped one in-wheel motor with every wheel, and Luciole [7] has one for each rear wheel. With independently controlled wheels, more effective chassis motion control like Direct Yaw Moment Control(DYC) [8][9] will be available. Iwama [10] studied about DYC with a vehicle which has one engine for front tires and two motors for rear tires. These motors are not in-wheel type, however, the individual torque control of rear tires and DYC was still available.

With these advantage, the advanced motion control of electric vehicle. should be studied, however, there are quite few researches [11] [12]. For example, these three advantages above will be utilized in an integrated control of each wheel and chassis. The typical purpose of such control is to enhance the vehicle stability, and the typical target situation is that the "2 wheel motored" or "4 wheel motored" EV turns the curve on slippery road with braking. One of the problems in such situation will be the measurement of slip ratio.

In this paper, studies about novel skid detector are carried out. This method can detect skid of driven wheel only with the values of motor's current and rotating velocity. No information about wheel absolute velocity or vehicle chassis velocity is required. Therefore, this method is expected to improve the performance of anti skid control, which is cooperating with DYC. Skid avoidance method with this novel skid detector is also discussed and examined with simulations in the latter part of this paper.

II. Skid Detector without Wheel Absolute Velocity

In this section, novel method of skid detection is proposed. Ordinary, slip phenomena of wheel is observed with the slip ratio λ, defined as

$$\lambda = \frac{r\omega - V}{r\omega} \qquad (1)$$

for an accelerating wheel, where r, ω, V are the wheel radius, wheel rotating velocity and wheel absolute velocity. Note that λ is the slip ratio and s denotes Laplace operator in this paper. Most ABS's or TCS's calculate this slip ratio to detect the skid of wheel. In order

mate wheel absolute velocity or vehicle chassis speed. The vehicle chassis speed is sensed with measurement of chassis' acceleration, or computed with the velocity of non-driven wheels approximately. On the contrary, the proposed method can detect skid with only motor speed and motor torque as follows.

A. Linear Model for Slip Phenomena

To treat slip phenomena, simple one-wheel vehicle model (Fig. 1) is assumed. Motion equations of wheel and chassis in this model are

$$M_w \frac{dV_w}{dt} = F_m - F_d \qquad (2)$$

$$M \frac{dV}{dt} = F_d \qquad (3)$$

respectively, where

F_m motor torque (force equivalent);
F_d traction force;
M_w wheel inertia (mass equivalent);
M vehicle weight;
V_w wheel rotating velocity (velocity equivalent);
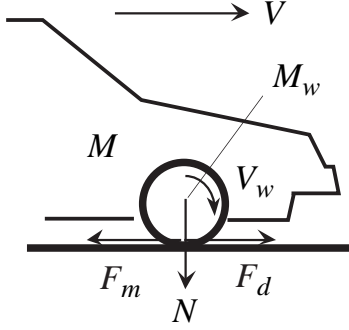V vehicle velocity.

Fig. 1. One wheel vehicle model.

F_d is the traction force, or friction force between the road and wheel. The normalized traction force μ is defined as the ratio of traction force F_d and normal force N on driven wheel,

$$\mu \equiv \frac{F_d}{N}. \qquad (4)$$

A plot of the normalized traction force μ versus the slip ratio λ shows a significant nonlinear characteristic which depends on the road conditions. Fig. 2 plots examples of $\mu - \lambda$ curves for various road conditions, dry asphalt, wet asphalt and ice.

The slip phenomena can be described with (1), (2)-(4) and $\mu(\lambda)$ function. Here, the following perturbation system is derived from these equations:

$$\Delta \lambda = \frac{\partial \lambda}{\partial V} \Delta V + \frac{\partial \lambda}{\partial V_w} \Delta V_w$$

$$= -\frac{}{V_{w0}} \Delta V + \frac{}{V_{w0}^2} \Delta V_w, \qquad (5)$$

$$M_w \frac{d}{dt} \Delta V_w = \Delta F_m - \Delta F_d, \qquad (6)$$

$$M \frac{d}{dt} \Delta V = \Delta F_d, \qquad (7)$$

$$\Delta F_d = N \Delta \mu = N \frac{\partial \mu}{\partial \lambda} \Delta \lambda$$

$$= a N \Delta \lambda, \qquad (8)$$

where $V_{\omega 0}$ and V_0 are the wheel and vehicle velocity at the operational point. The $\mu - \lambda$ characteristic is represented with a, the gradient of $\mu(\lambda)$ curve, defined as

$$a \equiv \left. \frac{\partial \mu}{\partial \lambda} \right|_{\lambda_0}, \qquad (9)$$

where λ_0 is the slip ratio at the operational point.

From (6)-(8), the transfer function from the motor torque F_m to the traction force F_d is finally given by

$$\frac{\Delta F_d}{\Delta F_m} = K \frac{1}{\tau_a s + 1}, \qquad (10)$$

where the proportional gain K and time constant τ_a are given by

$$K = \frac{M(1 - \lambda_0)}{M_w + M(1 - \lambda_0)}, \qquad (11)$$

$$\tau_a = \frac{M_w V_{w0}}{aN} \frac{M(1 - \lambda_0)}{M_w + M(1 - \lambda_0)}. \qquad (12)$$

Here we set some $\mu - \lambda$ curve as an example, which has its maximum μ at $\lambda = 0.1$. Then calculate K and τ_a with this $\mu - \lambda$ curve, and plot them versus λ in Fig. 3. As (11), (12) and Fig. 3 show, these values depend on λ as

$$K \simeq \frac{M}{M_w + M} \qquad \text{for small } \lambda \text{ (adhesive region)},$$
$$\tau_a \ll 1 \qquad \text{for small } \lambda \text{ (adhesive region)},$$
$$\tau_a \gg 1 \qquad \text{when } \lambda \to 0.1 \text{ (adhesive limit)},$$
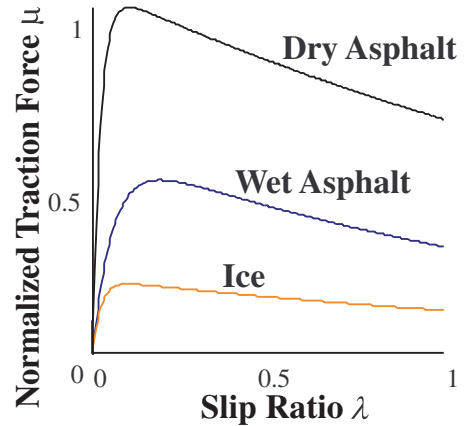$$\tau_a < 0 \qquad \text{when } \lambda > 0.1 \text{ (skid region)}.$$

Fig. 2. Normalized traction force μ plotted vs. slip ratio λ ($\mu - \lambda$ curve).
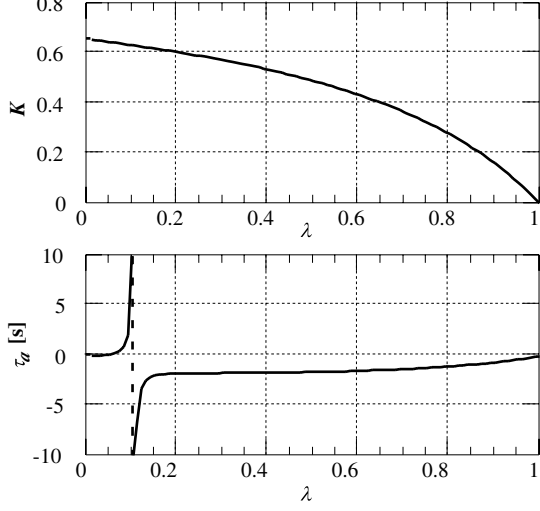
Fig. 3. Examples of K and τ_a.

B. Design of Skid Detector

Consequently, we roughly describe these properties of slip phenomena as

$$
\begin{cases}
\dfrac{\Delta F_m}{\Delta F_d} = \dfrac{M}{M_w + M} & \text{(in adhesive region)}, \\[2ex]
\dfrac{\Delta F_m}{\Delta F_d} \le 0 & \text{(in skid region)}.
\end{cases} \tag{13}
$$

Based on these simple descriptions, we suppose that the gradient of $F_m - F_d$ curve g,

$$
g \equiv \frac{dF_d}{dF_m}, \tag{14}
$$

indicates the status of slip phenomena as

$$
\begin{cases}
g \simeq \dfrac{M}{M_w + M} & \text{(in adhesive region)}, \\[2ex]
g \le 0 & \text{(in skid region)}.
\end{cases} \tag{15}
$$

Note that g for adhesive wheel only depends on the vehicle weight and wheel inertia in this description.

To apply this method, the value of traction force F_d is required. Now we are concerning about EV, or concerning about electric motor. Therefore, usual disturbance observer(DOB) has enough performance to estimate F_d as a disturbance or load torque[1] [13]. We call this estimator "traction force observer". Note again that it is quite easy to get the accurate value of motor torque.

III. Experimental Results of Skid Detector

A. Experimental Results on Asphalt Road

The proposed skid detector is applied to the experimental data obtained with the laboratory-made experimental EV "UOT Electric March I". Fig. 5 is the photo of "UOT Electric March I", and Table I shows the specifications of this vehicle. This EV has one DC motor in stead of an engine, as figured in Fig. 6. The motor torque is transmitted to the front wheels through clutch, reduction gears, and driving shaft. Details of
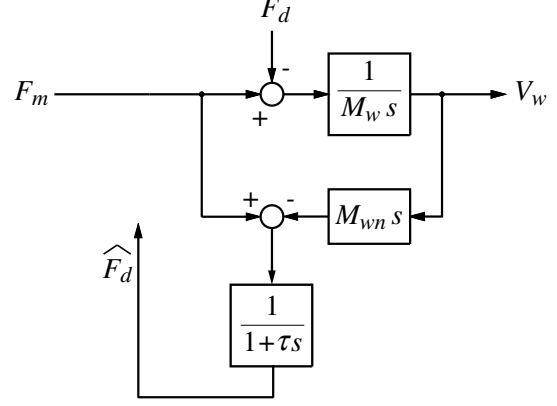

Fig. 4. Block Diagram of Disturbance Observer.

this vehicle are described in [1]. Since each rotating velocity of front and rear wheel is measured with shaft encoder, slip ratio λ can be calculated as a reference value. To measure λ, only longitudinal experiments are carried out in this paper.

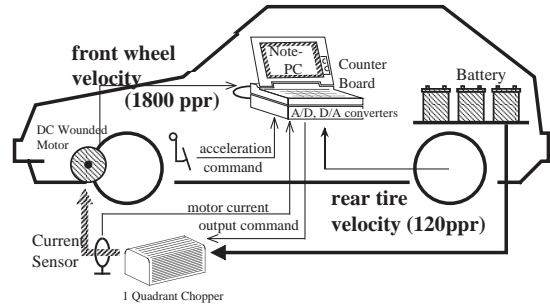Fig. 5. Laboratory-made EV "UOT Electric March I"

Fig. 6. Configuration of UOT Electric March I

Fig. 7 plots the time evolution of slip ratio λ for driven wheel, when the EV accelerated on the dry asphalt. From this figure, the driven wheel is estimated to be skidding between 1-2[s]. Fig. 8 shows the time response of F_m and traction force $\hat{F}_d$. $\hat{F}_d$ is observed with traction force observer, mentioned above, which has a time constant of 100[ms]. Fig. 9 shows the $F_m - F_d$ curve obtained in this experiment. Recursive least square (RLS) method was applied with forgetting fac-

Motor	DC Motor
Rated Power	
1 hour	20.8[kW] (28.3[HP])
5 min.	32.5[kW] (44.3[HP])
Torque Const.	0.2122[Nm/A]
Max. Torque	85[Nm]
Gear Ratio*1	13.5

Battery	Lead Acid
Nominal Capacity	92[Ah]
Weight	27.5[kg](for 1 unit)
Total Volt.	120[V] (with 10 units)

Chassis	Nissan March
Size	$3785 \times 1560 \times 1395$ [mm]
Weight	1000[kg]*2
Wheel Inertia	21.1[kgm²]*3
Wheel Radius	0.26[m]

CPU	i386, 20[MHz]
Encoder	1800[ppr](front wheel)
	120[ppr](rear wheel)

*1 ... Value in the all experiments.
*2 ... Including motor, batteries, etc.
*3 ... Including the rotor of motor, affected by gear ratio.
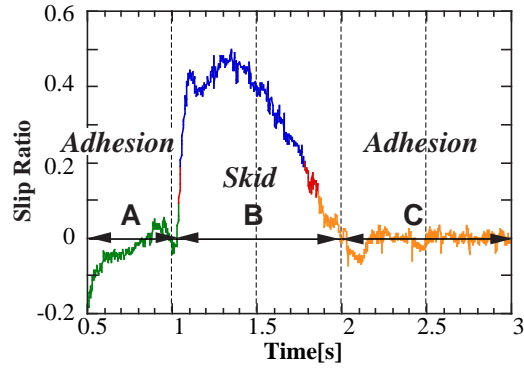
TABLE I
SPECIFICATIONS OF "UOT ELECTRIC MARCH I"

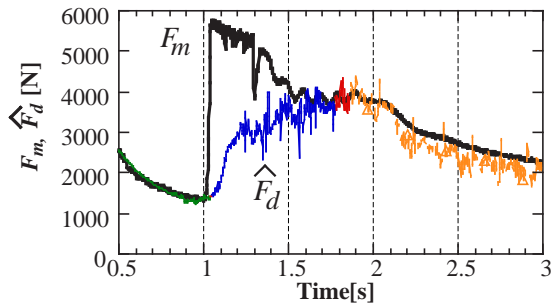Fig. 7.   Slip ratio (experiment on dry asphalt).

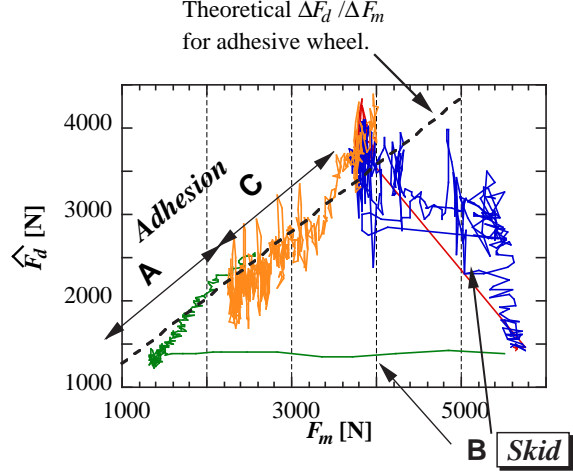Fig. 8.   Time response of F_m and F_d (experiment on dry asphalt).
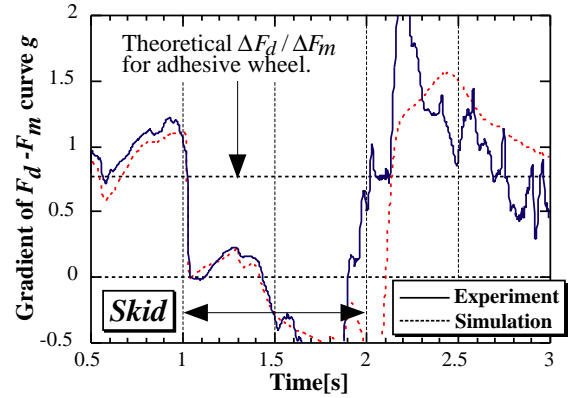

Fig. 9. F_m-F_d curve (experiment on dry asphalt).

Fig. 10. g, the gradient of F_m-F_d curve(experiment on dry asphalt).

tor to calculate the gradient g of this curve. Calculated g is plotted in Fig. 10. Dashed lines in Fig. 9 and Fig. 10 indicate the theoretical gradient for adhesive wheel calculated in (15). As Fig. 10 shows, the gradient g is about 0 or negative value when the wheel is skidding. In contrast, g is near or above the theoretical value for adhesive wheels, when the wheel is adhesive. These figures show the effectiveness of proposed skid detector, which sense the skid with g, the gradient of $F_m - F_d$ curve.

B. Experimental Results on snowy road

Another experiment was carried out with more slippery road condition. Fig. 11 shows the time evolution of slip ratio λ, when the EV "UOT Electric March I" accelerated on the snowy road. Fig. 11 indicates that the driven wheel was skidding between 0.5-3[s]. Fig. 12 shows the gradient g of the $F_m - F_d$ curve, identified with RLS method. As same as the previous case, g takes about 0 or negative value for skidding wheel, and is nearly equal to its "adhesive" value (dashed line) for adhesive wheel. Therefore, the skid detector can sense the skid of wheel with the immediate drop of g. These experimental results for snowy road also indicate the
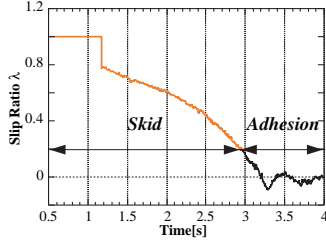
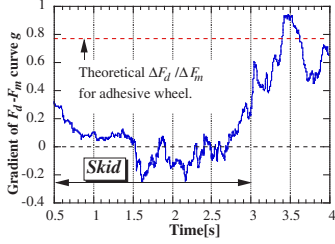Fig. 11.   Slip ratio (experiment on snowy road)

Fig. 14.   Slip ratio (experiment on wet iron plate.)

Fig. 12. g, the gradient of F_m-F_d curve(experiment on snowy road).
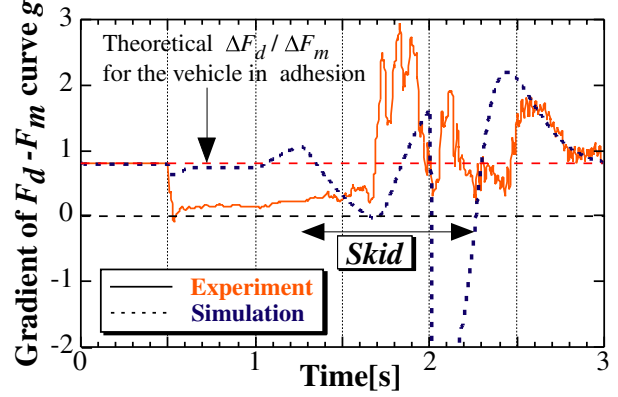
Fig. 15. g, the gradient of F_m-F_d curve(experiment on wet iron plate).

C. Experimental Results on Wet Iron Plate

Here we describe the experimental results on wet iron plate(Fig. 13). First, the "UOT Electric March I" was running on the dry asphalt, keeping its motor torque to constant value. Then the vehicle reached to the iron plate of 0.8 [m] wide, and then the wheels started to skid. Fig. 14 indicates this skid growth with the time response of slip ratio. The proposed skid detector was applied, and Fig. 15 shows the results of the skid detection. As these figures show, the proposed method could not detect the skid properly. This problem is caused by the small variation of motor torque F_m. The proposed detector sense the skid with the drop of $\Delta F_d/\Delta F_m$, thus it is difficult to identify this gradient when ΔF_m is too small. Modification of proposed skid detection algorithm is required, to make it stable even when the motor torque F_m does not vary. It seems to be possible since F_d still varies in this situation, however, this still remains for the further studies.
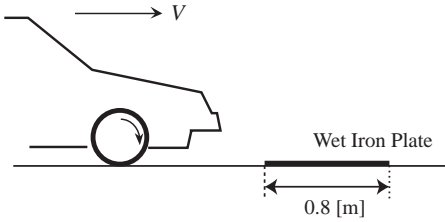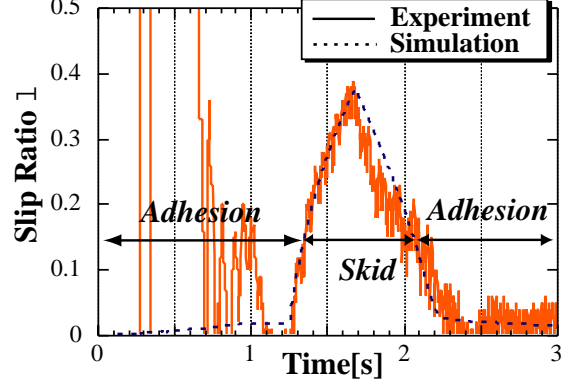

Fig. 13.   Slip Experiments on wet iron plate.

IV. Simulation Results of Skid Prevention with Skid Detector

In this section, some simulation results are described to show our basic idea of how to prevent skid with proposed skid detector. The output of the skid detector is g, defined with (14) in the previous section. Following (13), we change the control status depending on g,

$$
\begin{cases}
g > 0.4\gamma_M & : \text{adhesive status,} \\
g \le 0.4\gamma_M & : \text{skid status,} \\
g \ge 1.2\gamma_M & : \text{re-adhesive status,}
\end{cases}
\tag{16}
$$

where

$$
\gamma_M = \frac{M}{M_w + M}.
\tag{17}
$$

In this simulation, the motor torque increases until the skid detector senses the wheel skid. Once $g < 0.4\gamma_M$, motor torque decreases until the status comes to be re-adhesive, or g grows up over $1.2\gamma_M$. This control algorithm in this simulation can be simply described as

$$
\begin{cases}
\dfrac{dF_m}{dt} = a & : \text{in adhesive / re-adhesive status,} \\
\dfrac{dF_m}{dt} = -a & : \text{in skid status.}
\end{cases}
\tag{18}
$$

In this simulation a is 240 [Nm/s], however, this value is just an example and not optimized in any meanings.

controller. This simulation was carried with one-wheel vehicle model (2), (3), with additional air and running resistance terms. The $\mu-\lambda$ curve is modeled with Magic Formula tire model, which has its peak value $\mu = 0.6$ at $\lambda = 0.1$. The parameters in these simulations are the same as in Table I. As shown in Fig. 16, motor torque F_m increases at first, then the slip ratio λ increases. When the λ becomes larger than 0.1, the wheel skidding is sensed by the skid detector with short time delay, and the controller decreases motor torque F_m until the skid detector senses re-adhesion. In result, the slip ratio λ oscillates around 0.1, as shown in Fig. 16 (c). Fig. 17 is the results of same simulation with different $\mu - \lambda$ curve. The peak μ is 0.4 at $\lambda = 0.2$. In this case, the slip ratio varies around $\lambda = 0.2$.

These results indicate that

1. serious skid can be avoided,
2. and the driving force F_d varies around its maximum value.

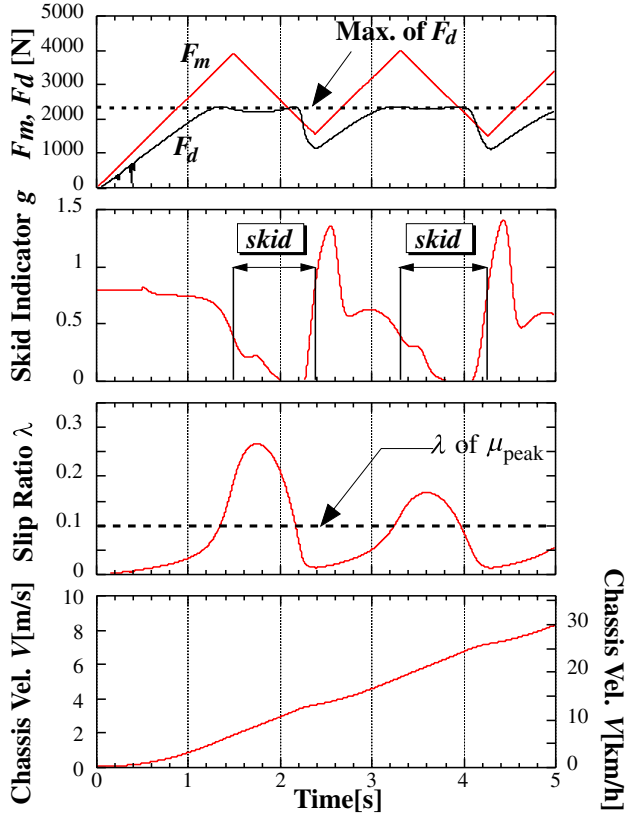Therefore, these results indicate the effectiveness of the proposed skid detector for anti skid control.

Fig. 16. Simulation results of skid prevention with proposed skid detector. μ's peak is at $\lambda=0.1$.

V. Conclusions

In this paper, novel skid detection method for electric vehicle (EV) was proposed and discussed. This proposed method can detect skid of wheel with only the values of current and rotating velocity of each motor, in other words, with only the information of motor itself. Estimation of vehicle chassis velocity or wheel
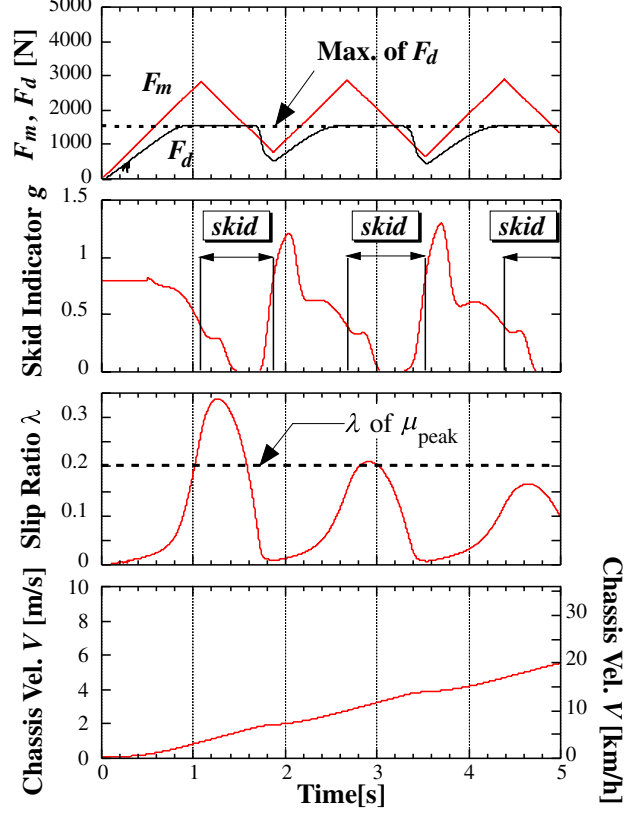

Fig. 17. Simulation results of skid prevention with proposed skid detector. μ's peak is at $\lambda=0.2$.

absolute velocity is not required any more, and this is remarkable advantage over conventional methods.

In this proposed method, traction force is estimated with simple "traction force observer", thus the exact value of shaft input torque is required. It is quite easy in EV. As we pointed out, this is one of the advantages of EV for vehicle motion control.

The proposed algorithm was examined experimentally with laboratory-made electric vehicle "UOT Electric March I". These experimental results show the effectiveness of proposed skid detection method. Simple simulation was also carried out to confirm the effectiveness of the proposed skid detector in anti skid control. These results show that serious skid can be prevented with proposed skid detector. More detailed studies about the design of controller are required. Demonstrations with experiments will be also carried out.

Proposed skid detector requires no information about vehicle chassis velocity or slip ratio, thus this method should be significantly effective for skid avoidance during the cornering motion. This anti skid controller will be integrated and examined with our new experimental EV "UOT Electric March II" (Fig. 18) [14], which has independently controlled four in-wheel motors. Cooperative control of proposed skid avoidance method and DYC, control of vehicle chassis motion with torque difference, still remains for further studies. It will be studied experimentally with our new EV.
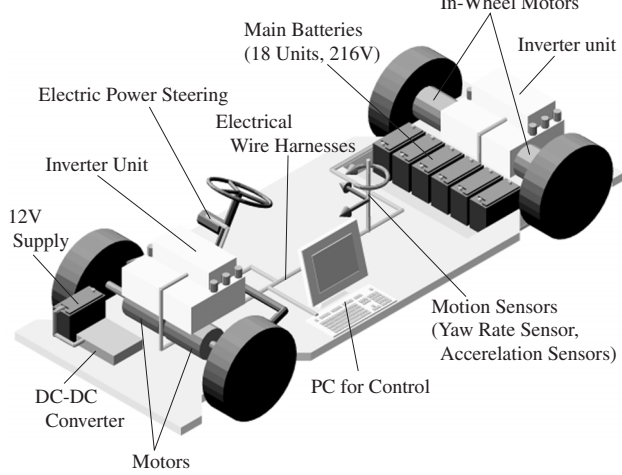
Fig. 18. Configuration of our new EV.

REFERENCES

[1] Y. Hori, Y. Toyoda, and Y. Tsuruoka, "Traction control of electric vehicle: Basic experimental results using the test EV "UOT electric march"," *IEEE Trans. Ind. Applicat.*, vol. 34, no. 5, pp. 1131–1138, 1998.

[2] U. Kiencke and A. Daiss, "Observation of lateral vehicle dynamics," *Control Eng. Practice*, vol. 5, no. 8, pp. 1145–1150, 1997.

[3] Fredrik Gustafsson, "Monitoring tire-road friction using the wheel slip," *IEEE Control Systems Magazines*, vol. 18, no. 4, pp. 42–49, 1998.

[4] Fredrik Gustafsson, "Slip-based tire-road friction estimation," *Automatica*, vol. 33, no. 6, pp. 1087–1099, 1997.

[5] T. Ashikaga, M. Mori, T. Mizuno, K. Nagayama, T. Kobayashi, and T. Kubo, "High efficiency induction motor control method for electric vehicle," in *Proc. IPEC'95*, Yokohama, 1991, pp. 113–118.

[6] H. Shimizu et al., "The concept and simulation of a high performance EV IZA," in *Proc. EVS. 11 no.5,*, 1992.

[7] H. Shimizu, J. Harada, C. Bland, K. Kawakami, and C. Lam, "Advanced concepts in electric vehicle design," *IEEE Trans. Ind. Electron.*, vol. 44, no. 1, pp. 14–18, 1997.

[8] Yasuji Shibahata et al., "The improvement of vehicle maneuverability by direct yaw moment control," in *Proc. AVEC '92*, 1992, number 923081.

[9] M. Abe et al., "Estimation of vehicle side-slip angle for DYC by using on-board tire model," in *Proc. 4th International Symposium on Advanced Vehicle Control*, Nagoya, 1998, pp. 437–442.

[10] Norio Iwama, Yukio Inaguma and Katsuhiro Asano, "Active control of an automobile -independent rear wheel torque control-," *SICE*, vol. 28, no. 7, pp. 844–853, 1992. [In Japanese]

[11] P.Khatun, C.M.Bingham, P.H.Mellor, and N.Schofield, "Discrete-time ABS/TC test facility for electric vehicles," in *Proc. EVS. 16*, Beijing, 1999, p. 75.

[12] Y. Wang and M. Nagai, "Integrated control of four-wheel-steer and yaw moment to improve dynamic stability margin," in *Proc. 35th IEEE Conf. Decision and Control*, Kobe, 1996, pp. 1783–1784.

[13] K. Ohishi, K. Nakano, I. Miyashita, and S. Yasukawa, "Anti-slip control of electric motor coach based on disturbance observer," in *Proc. 5th Advance Motion Control*, Coimbra, 1998, pp. 580–585.

[14] Shin-ichiro Sakai, "Project of motion control in an electric vehicle with four in-wheel motors," URL: http://www.hori.t.u-tokyo.ac.jp/997/sakai/Research/index.html, 1999.